
Article:
Lai, F., Qu, S., Duan, Y. et al. (6 more authors) (2018) The wear and fatigue behaviours of hollow head & sodium filled engine valve. Tribology International, 128. pp. 75-88. ISSN 0301-679X

https://doi.org/10.1016/j.triboint.2018.07.015

Accepted Manuscript

The wear and fatigue behaviours of hollow head & sodium filled engine valve

Fuqiang Lai, Shengguan Qu, Yong Duan, Roger Lewis, Tom Slatter, Lianmin Yin, Xiaoqiang Li, Huahuan Luo, Ge Sun

PII: S0301-679X(18)30343-8

DOI: 10.1016/j.triboint.2018.07.015

Reference: JTRI 5309

To appear in: *Tribology International*

Received Date: 28 March 2018

Revised Date: 6 July 2018

Accepted Date: 9 July 2018

Please cite this article as: Lai F, Qu S, Duan Y, Lewis R, Slatter T, Yin L, Li X, Luo H, Sun G, The wear and fatigue behaviours of hollow head & sodium filled engine valve, *Tribology International* (2018), doi: 10.1016/j.triboint.2018.07.015.

The wear and fatigue behaviours of hollow head & sodium filled engine valve

Fuqiang Lai[1,2], Shengguan Qu[1*], Yong Duan[1], Roger Lewis[2], Tom Slatter[2], Lianmin Yin[1], Xiaoqiang Li[1], Huahuan Luo[3], Ge Sun[3]

(1. School of Mechanical and Automotive Engineering, South China University of Technology, Guangzhou 510640, Guangdong, China

2. Department of Mechanical Engineering, The University of Sheffield, Mappin Street, Sheffield, UK, S1 3JD

3 Huaiji Dengyun Auto-parts (Holding) CO., LTD. Huaiji County 526400, Guangdong, China)

Abstract:

Increasing performance requirements of IC engines often leads to higher combustion chamber temperatures that cause premature failure of exhaust valves. This paper presents a tribological assessment of hollow head & sodium filled valves (HHSVs) produced using a new manufacturing process. Tests were conducted using bespoke bench-top wear and fatigue apparatus, and the HHSV specimens survived defined durability tests. When compared to traditional solid valves, the highest temperature of the hollow stem & sodium filled valves decreased from 745 °C to 590 °C. It was established that the new process did not adversely affect the wear mechanisms (oxidation accelerated adhesion) and the material loss magnitude when compared to solid valves. The design of HHSVs tested gives a 16.1% reduction in mass.

Key words: hollow head engine valve; wear testing; fatigue behaviour; wear mechanism

Corresponding Author*: Shengguan Qu, Professor; E–mail: qusg@scut.edu.cn; Tel:+86-020-87111983.

1. Introduction

The valvetrain is one of the most important systems in an internal combustion engine (ICE), as it controls the gas flow and the timing of the engine. The valve and valve seat insert are critical components of the valve train, because they control the entry of air (and in some designs, fuel), the output of exhaust gas, and provide sealing during the compression and combustion processes [1]. One of the primary targets in the combustion engine industry is the increase of the engine power to size ratio. Certain higher performance engines need higher temperature capable valve materials due to increased exhaust gas temperatures, higher exhaust flow rates, and higher in-cylinder pressures. Consequently, engine components' thermal efficiency must be optimized.

In order to deal with the challenges of the use of new fuels, often directly injected, and the increased employment of turbo charging in the engine many new materials and products for engine valves and seat inserts have been developed. One emerging technology is that of sodium filled valves and these have been utilized in engines significantly increased in recent years [2]. Two main types of sodium filled engine valves have been developed to date: the hollow stem sodium filled valve (HSV) and the hollow head & sodium filled valve (HHSV) [2–5]. Compared to conventional solid engine valves, sodium filled valves have two distinct advantages: a reduction in valve mass and reduction in the sustained temperatures experienced in the bulk material of the valve. In addition, particularly for gasoline engines, sodium filled valves are beneficial to improving an ICE's knock behaviour through decreasing exhaust valve bottom temperatures, leading to an improvement for engine fuel consumption and valve train durability [5]. For instance, Colwell researched the temperature reduction effect for the two types of

sodium filled valves (HSV and HHSV) compared to the solid valve [3]. The research results revealed that the inner filled sodium significantly decreased the valve temperature, and the hollow head valve had an apparently better performance than the hollow stem valve in its cooling effect. In a hollow stem sodium filled valve, the sodium occupies about 60% of the hollow space. The melting temperature of sodium is approximately 97.7 °C, so sodium would turn to liquid state at high temperature as the engine was running. The sodium would move up and down in the hollow space following the motion of valves. Thus, more heat could be transferred from the head to the stem. Then, the heat was transferred to the cooling system through the valve guide, so the valve temperature value could be reduced. Lowering valve temperature by only a slight amount may take it out of the critical range for failure for the component. Furthermore, because it eliminates the need for expensive heat-resistant materials, costs can be reduced.

A mass comparison of solid valves and three different types of sodium filled valves was reported by Hu [4] where compared to a solid valve, the mass of a HSV and a HHSV were decreased to 93 % and 84 %, respectively. Although the valves' mass is a small proportion in an ICE, they occupy a large proportion in the valve train system and reducing their mass is markedly helpful to optimize the dynamic characteristic of the system. Additionally, the impact seating forces of the valves and seat inserts would be decreased with the mass reduction of valves. Consequently, it certainly is a beneficial relief for the severe work conditions of valves and seat inserts.

This paper presents a novel manufacturing method for HHSVs with stellite hardfacing, and a study of their tribological and durability performance. A summary of the work and its presentation in this paper is shown in Fig. 1. At first, a traditional solid exhaust valve of a

natural gas fuelled diesel was selected and its geometry information was identified. Then, this type of exhaust valve was redesigned and manufactured to be a hollow head and sodium filled valve through a novel potential manufacturing method. Subsequently, durability tests of the HHSV specimens and the original solid valve were performed to evaluate the durability of the hollow head and the wear resistance of the valve seating face. The durability tests were conducted without lubrication using bespoke bench-top wear and fatigue apparatus. The tested valve specimens and the matched seat inserts were characterized using scanning electron microscopy (SEM), an energy–dispersive spectroscopy (EDS), optical microscopy and a profilometer. The wear resistance of the tested valves and seat inserts was compared and the wear mechanisms were analyzed. Furthermore, stress analysis of the HHSV specimens during the durability tests was carried out using a Finite Element Method (FEM). Simultaneously, a rotating bending fatigue tester was applied to evaluate the fatigue strength of the materials used for the HHSVs. In addition, hardness measurements were used to estimate the testing temperatures of the solid valve and HSV in a real gasoline engine. Based on the above test results, an overall assessment of the HHSV was obtained.

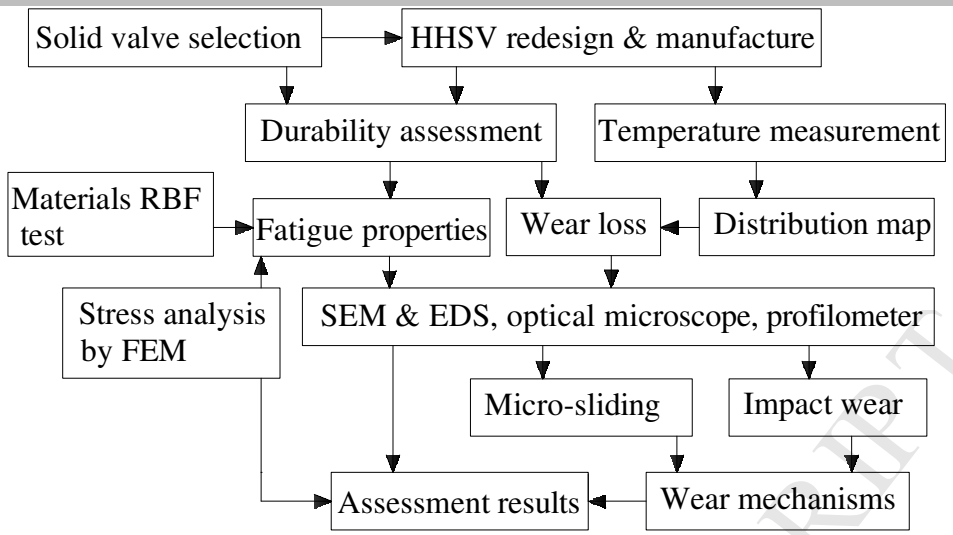

Fig. 1 The flow chart of the research.

2. Manufacturing method

2.1 A review of manufacturing methods

Despite the development of high temperature alloys, effective cooling techniques were still needed for aircraft piston engine valves [6,7]. Mercury, nitrate salts and sodium were all once utilized as coolants in the hollow valve and the sodium became the predominant solutions with its low melting point and density as well as high thermal conductivity. Sodium filled valves were first invented for piston aircraft engines to resist the high temperature work conditions as the liquid sodium cooling dissipated the heat during engine operation significantly better than previous designs [8]. This type of valve cooling design was then introduced to the automotive ICEs, initially for the exhaust valves in heavy duty diesels.

Many researchers have put forward different types of manufacture methods. Wang introduced two forging manufacture methods for HHSV [9]. The first method processed the workblank through a valve hammer, before the hollow chamber was fabricated by machining. The main

steps of the valve hammer method were as follows: (1) workblank preparation; (2) die forging; (3) flash removal; (4) hollow chamber machining; (5) valve stem extension forging; (6) valve stem extension forging and sealing; (7) valve hollow stem drilling; (8) valve stem forging and stem end sealing. The second method utilized a valve forging machine to produce the initial hollow chamber through several forging processes and a subsequent machining process. The main steps of the valve forging machine method were as follows: (1) workblank preparation; (2) workblank upsetting; (3)-1 punching forming; (3)-2 hot rolling on the valve wall; (3)-3 head upsetting. The steps (4) to (8) of the valve forging machine method were the same as the valve hammer method. However, these methods are only suitable for valves with large dimensions. As described by Wang [9], valve head diameter is approximately 70 mm and valve stem diameters is 20 mm.

MAHLE has developed a type of HHSV based on HSV with cylindrical bores [10]: with one additional process: electrochemical machining. Additionally, the hollow cavity volume could be extended further. Taking advantage of the recent developments in additive manufacturing processes, Cooper et al. designed and manufactured hollow engine valves by Additive Layer Manufacturing (ALM) [11]. Although ALM could manufacture hollow head valves with any designed shape, this manufacturing process is significantly much too expensive for mass production. Compared to the forging steels, the material performance fabricated by ALM should be researched and improved further.

2.2 The utilized manufacturing method

The most critical point for commercially successful manufacture of a hollow head valve is

sealing the hollow head through a highly efficient and low cost technology. Over the past several years, Huaiji Dengyun Auto-parts (Holding) CO., LTD had developed and refined a new manufacture method to seal the hollow head by welding friction [12]. The welding method for sealing the valve hollow head have variously included electro-welding [4], laser beam welding and friction welding. A novel practical HHSV manufacturing method named the "drilling plus friction welding method", based on drilling and friction welding technology, was put forward in this work, as presented in Fig. 2. The method has seven steps, as follows: (1) solid bar workblank preparation; (2) upsetting; (3) punching for valve hollow head; (4) valve hollow stem drilling; (5) friction welding sealing at valve hollow head; (6) sodium filling and friction welding sealing at valve hollow stem; (7) seating face hardfacing with Stellite alloy.

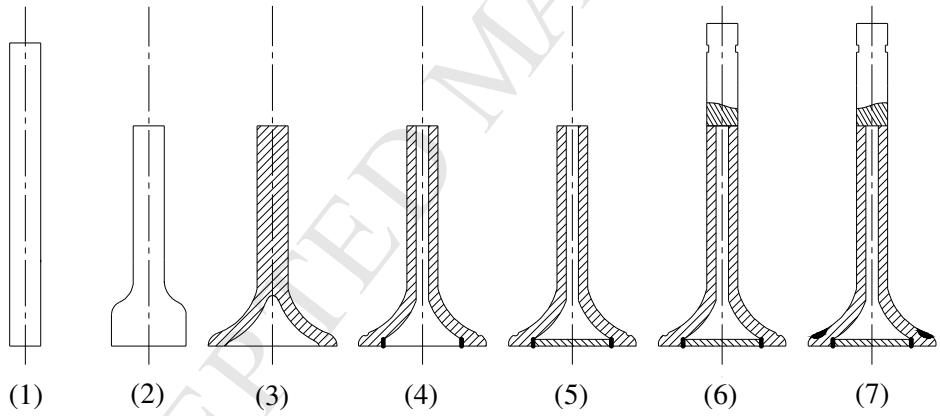

Fig. 2. Manufacturing process of hollow head & sodium filled valve.

The fifth step is the critical step, where the valve hollow head is sealed with the disk conical surface through friction welding. Selected images of the process are recorded in Fig. 3. The friction welding process was optimized to hold high quality, stability and productivity, and low cost.

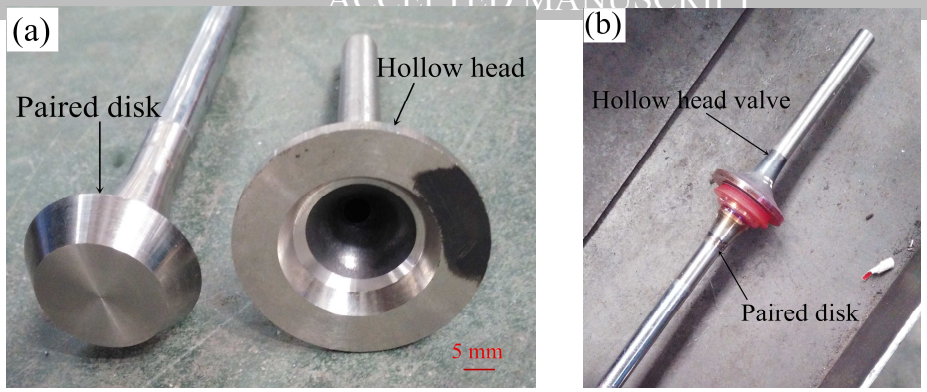

Fig. 3. Manufacturing progress records.

After the friction welding process, the HHSVs were annealed to release the residual stress. Some HHSVs were sectioned and polished for junction surface integrity analysis, as presented in Fig. 4(a–d). The gaps near the edge shorter than 0.3 mm. The hardness across the friction welding heat affected zone is presented in Fig. 4(e), indicating that the materials across the friction welding area had similar properties. It should be noted that, if hollow head valves are to be used in firing ICEs, it is necessary to insure the durability of the welds that are exposed to combustion and this work is described later in section 3 and 4.

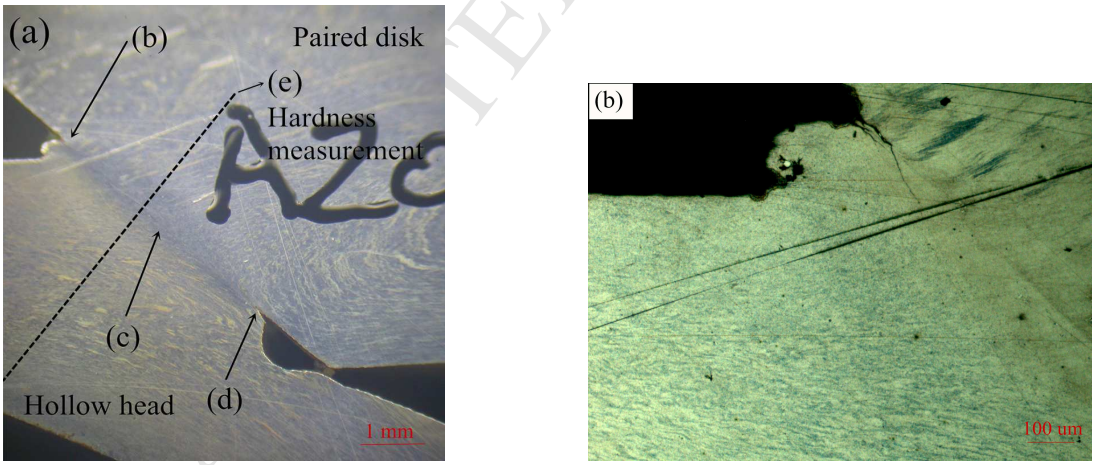

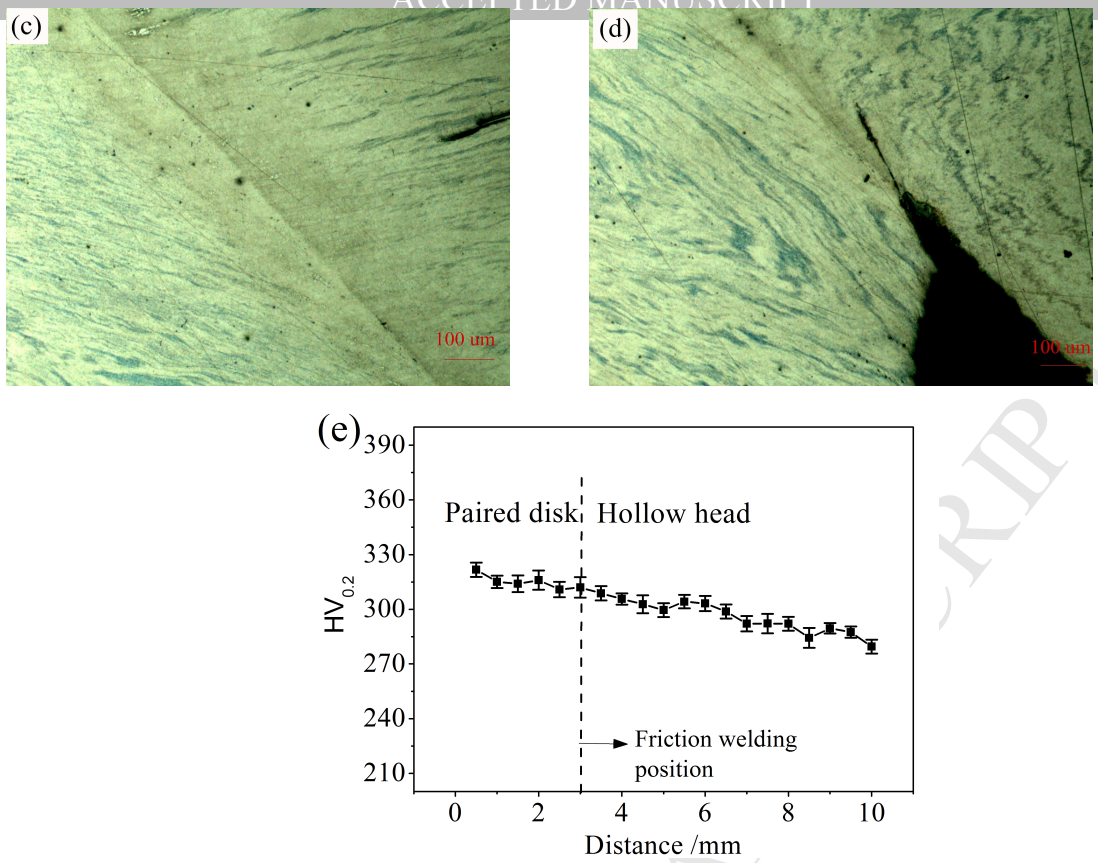

Fig. 4 (a–d) Junction surface detection after friction welding process; (e) hardness across the friction welding heat affected zone .

3. Experimental details

3.1 Materials and HHSV specimen preparation

Engine valves are usually manufactured from iron-, nickel-, and cobalt-based metallic alloys. In general, martensitic steels are used for intake valves, austenitic alloys and super alloys are used for exhaust valves. Austenitic alloys 3Cr23Ni8Mn3N (23-8N) and 61Cr21Mn10Mo1V1Nb1N (X60) are commonly used for exhaust valves in modern engines. The main chemical compositions of engine valve steels, hardfacing alloy and seat insert are presented in Table 1. The engine valve steel was provided by the steel manufacturer following Chinese Standard GB/T 23337-2009 (Internal combustion engines- Intake and exhaust valves- Specification).

Microstructure of the steel is presented in Fig. 5. Most grain diameter of 23–8N steel specimen is 0.5-10 μm, while most grain diameters of X60 steel specimen is 0.3-3 μm. Table 2 reveals the mechanical properties of 23–8N steel at room temperature and 650 °C.

Table 1 Compositions of the engine valve specimens and seat inserts (wt. /%).

Steel	C	Si	Mn	Ni	Cr	W	N	Mo	V	Nb	Fe	Co
23–8N	0.32	0.81	2.01	7.15	22.45	–	0.31	0.001	–	–	Bal.	–
X60	0.65	0.21	10.40	0.45	20.65	–	0.37	0.79	0.79	1.06	Bal.	–
42Cr9Si2	0.42	2.38	0.48	0.17	8.4	–	–	–	–	–	Bal.	–
45Cr9Si3	0.44	2.92	0.33	0.15	8.58	–	–	–	–	–	Bal.	–
Stellite F	1.5 –2.0	0.9– 1.3	≤0.50	21.0 –24.0	24.0 –27.0	11.5 –13.0	–	≤0.60	–	–	≤3.0	Bal.
Seat insert	0.75 –0.85	1.75 –2.25	0.20- 0.60	1.15 –1.65	19.0 –20.5	–	–	–	–	–	Bal.	–

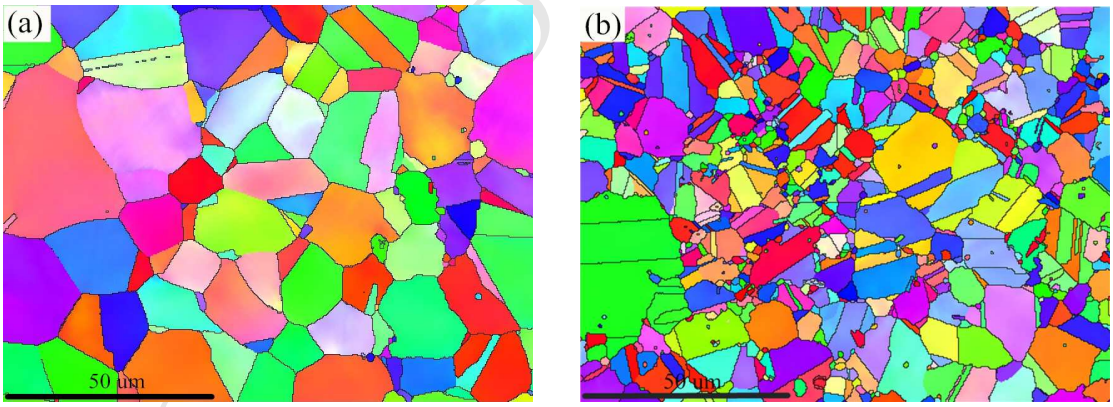

Fig. 5. Microstructure of the steel (EBSD): (a) 23-8N, (b) X60.

Table 2 Mechanical properties of 23–8N steel.

	σ_b at 25 °C	σ_s at 25 °C	E at 25 °C	σ_b at 650 °C	σ_s at 650 °C	E at 650 °C
23–8N	1002 MPa	605 MPa	183 GPa	579 MPa	310 MPa	149 GPa

Based on the presented drilling plus friction welding method in Section 2.2, hundreds of HHSV specimens have been produced successfully. Three HHSVs and one solid valve were selected for later durability tests, and the properties of the four valves are listed in Table 3. It should be noted that valve 3 was from the original type of solid exhaust valve, and this type of valve is being used in a natural gas fuelled diesel.

The nitriding process was performed by salt bath liquid nitriding at 580 °C for 35 to 40 minutes. The hardfacing process on the valve seating face was performed on a Plasma Transferred Arc powder hardfacing machine (PTA-4). During the hardfacing process, the transferred arc voltage was 10.8 V, transferred arc current was 110–130 A , and the non-transferred arc current was 21–25 A. The supply speed of Stellite F powder was 4–5 g/min, and the thickness of the resulting hardfacing material was 1.1–1.4 mm. After the hardfacing process, the HHSVs were cooled to the room temperature in the atmosphere. The hardness of Stillite F alloy is 424.4±4.3 $HV_{0.2}$.

Table 3 Valve specimens properties.

Valve name	Valve type	Head material	Stem material	Seating face material	Valve weight (g)	Head material hardness ($HV_{0.2}$)
Valve 1	HHSV	23-8N	23-8N, nitriding	23-8N, nitriding	114.3	317.8±7.1
Valve 2	HHSV	23-8N	23-8N, nitriding	23-8N, nitriding	114.3	314.1±5.7
Valve 3	Solid	X60	X60, nitriding	X60, nitriding	138.2	400.5±5.6
Valve 4	HHSV	23-8N	42Cr9Si2, nitriding	Stellite F	115.9	313.4±4.6

3.2 Durability test for valve components

In order to verify the durability of the new structure and manufacturing process, three HHSVs and one solid valve were subjected to a bench-top fatigue/wear test using a special apparatus

developed for this purpose and presented in Fig.6 (a). Its detailed information can be seen in the work of Lai et al. [1]. The test schematic is illustrated in Fig.6 (b), the valve and seat insert geometry are presented in Fig.6 (c). One type of seat insert was used in the test, and the test conditions are presented in Table 4. Temperature was set at 650 °C, load frequency was 10 Hz, valve lift was 5 mm. No misalignment between valve and seat insert was used and the valve did not have any rotational motion during the test.

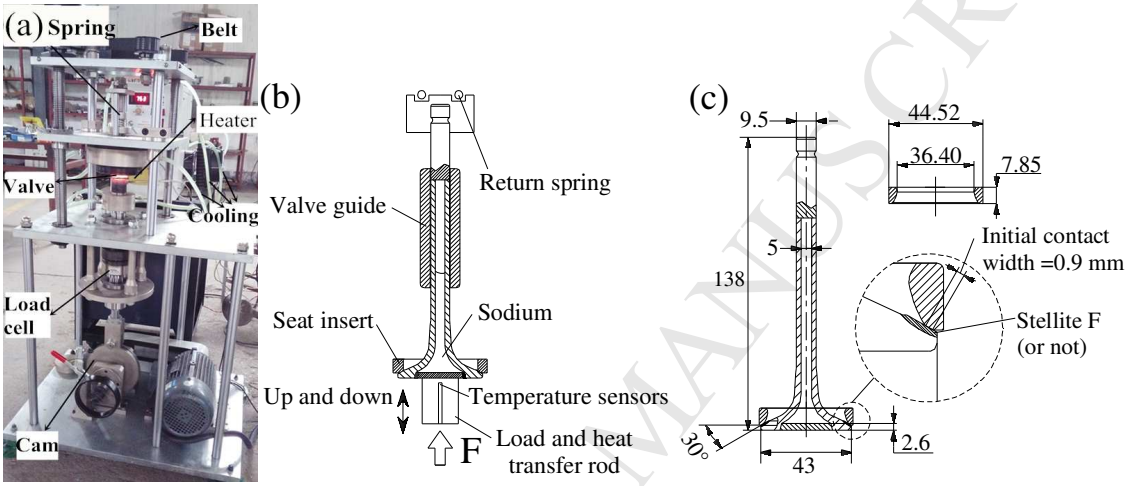

Fig. 6 (a) The designed apparatus [1]; (b) durability test schematic; (c) specimen geometry.

Table 4 Test conditions of the durability test.

Specimen No.	Valve type	Valve name	Seat insert name	Load (kN)	Contact pressure (MPa)
1	HHSV	Valve 1	Seat insert 1	10	56.62
2	HHSV	Valve 2	Seat insert 2	4.2	23.78
3	Solid	Valve 3	Seat insert 3	4.2	23.78
4	HHSV	Valve 4	Seat insert 4	4.2	23.78

Wear scar width measurement was conducted by means of a quantitative analysis previously used by other authors and commonly used in the literature [13-16]. During the test, the wear scar width of valve seating face and seat insert was measured by an optical microscopy with a

long-focus and a scaleplate, as presented in Fig. 7. After the test, a profilometer (Mahr XC20) was also utilized to measure the wear scar for valve seating faces and seat inserts. All the measurements were conducted at four points in the direction of circumference of the components at 90° intervals.

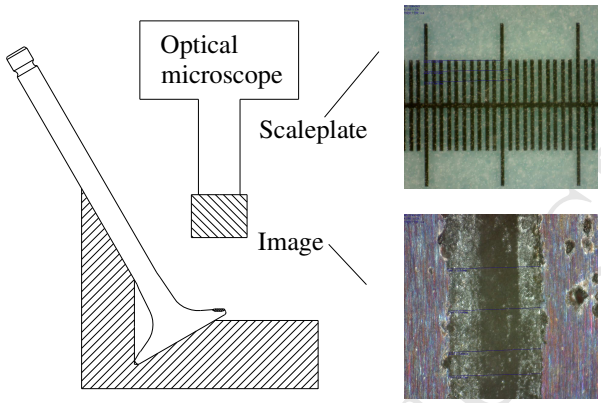

Fig. 7. Schematic of the measurement of valve wear scar width.

3.3 Stress analysis by FEM

The mechanical properties of the 23-8N steel at high temperature tensile test was performed by an ultimate tensile testing machine, and the results are presented in Table 2 in Section 3.1. According the geometry information of the HHSV, its three dimensions model of HHSV was established. Then, mechanical properties of 23–8N steel at 650 °C were used as inputs to the material properties of the FEM model, and the element size was set at 0.2 mm. Based on the force conditions of the HHSV specimens during the durability test, the FEM model was established as presented in Fig. 8, The constraints are presented by the triangular symbols pointing the constrained direction of the relevant node. The calculation work was done on ANSYS 14.0 software.

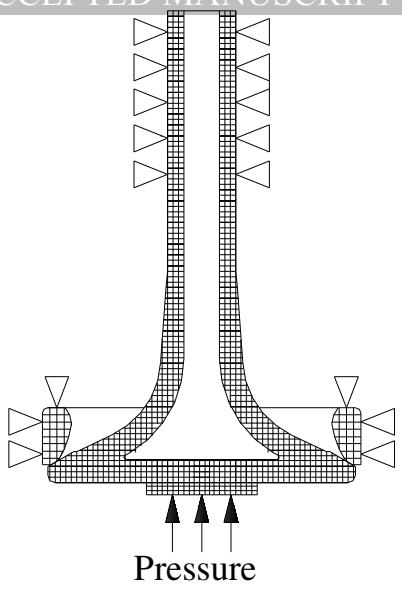

Fig. 8. Schematic diagram of HHSV FEM model.

3.4 Rotating bending fatigue (RBF) test for materials

In order to evaluate the fatigue performance of 23-8N steel at the elevated temperature, corresponding rotating bending fatigue (RBF) tests for material specimens were carried out with the group test method through a standard test rig as presented in Fig. 9. A RBF specimen was clamped in the furnace by the holder. Then, the RBF specimen was rotated by the motor under a constant applied bending moment. After a number cycles it would fracture, the fatigue life was recorded and obtained. Hence, the fatigue life of the material under different stress levels could be obtained. All RBF specimens were tested at 650 °C in ambient atmosphere with the stress ratio of $R = S_{\max} / S_{\min} = -1$, and a frequency of 100 Hz. When the cycles reached to ten million, the fatigue testing would be automatically suspended. It shoud be noted that the small hourglass shape material RBF specimens were used in the RBF test rig.

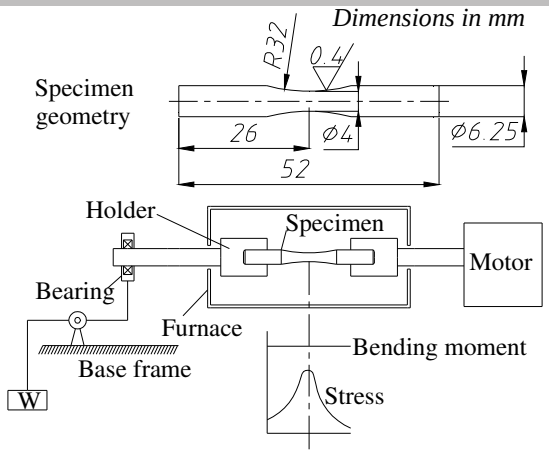

Fig. 9. Schematic diagram of RBF test and RBF specimen geometry.

3.5 Valve temperature measurement method

The work conditions around the exhaust valve of firing engine are severe for any measurement system. The valve temperature measurement methods include thermographic camera [17], thermocouples [10, 17-19] and hardness [20]. For smaller gasoline ICEs with small valve stem diameters, it is difficult to use thermocouple-based instrumentation and it is disproportionately time consuming. Furthermore, only a few thermocouples could be installed directly on a valve, leading to a single temperature could be measured at any one installation location. As for hardness method, a thermometric valve (TMV) made from special temperature sensitive valve steel was utilized. The steel was quenched and then cooled in cooling oil, it would maintain certain high hardness. Subsequently, if the steel was tempered at different temperatures, it would obtain the corresponding hardness. Generally, its hardness would change as a function of the maximum temperature it has been exposed to. Consequently, based on the steel hardness and temper temperature relationship curve, known as its calibration curve, if the steel hardness is measured, then the temper temperature could be derived. Although the hardness method is less accurate, in terms of absolute temperature values, it can easily provide a temperature map of the

entire exhaust valve and it is economical in time and cost [20].

In the paper, the TMVs were whole valves which were made from 45Cr9Si3 martensitic steel. The TMVs were quenched at 1030 °C and then cooled in oil, and the calibration curve of the steel is presented in Fig. 10. One TMV of a hollow stem valve and one TMV of a solid valve were assembled as exhaust valves in the same cylinder of a dynamometer gasoline engine. The engine operated at full speed for two hours at set engine operating conditions. Then, the two TMVs were taken out and sectioned.

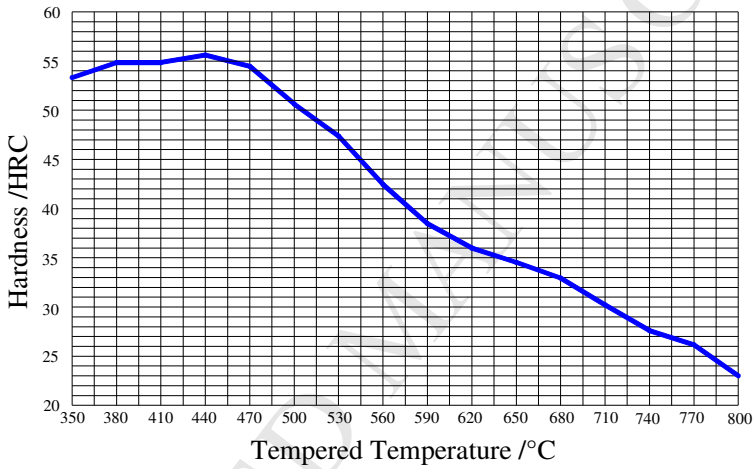

Fig. 10. The calibration curve of quenched 45Cr9Si3 steel.

4. Results and discussion

4.1 Temperature distributions

The temperature distributions of exhaust valves drawing from actual data for the two types of TMVs in a same cylinder are presented in Fig.11 and Table 5. It was found that the maximum temperature of the solid valve reached 745 °C, which appeared near the stem area at the concave area of valve. These results present similar temperature distribution trends as reported in previous research by Colwell [3] and Beerens et al. [10]. Owing to the fuel combustion in the

cylinder, the valve head was heated at high temperature. With the addition of the washout of the exhaust gas, the exhaust valve concave area suffered the maximum temperature.

The temperature of valve head centre were also high, the maximum temperature reached to 665 °C. In contrast, as for the hollow stem & sodium filled valve, the maximum temperature of the whole valve was 590 °C, and the hottest point shifted toward the head area. Compared to the solid valve, the maximum temperature reduction was 155 °C. In addition, the maximum temperature of HSV head centre was 581 °C, which was 84 °C lower than the solid valve head centre. It is therefore suggested that the heat in the valve head was conducted through the hollow stem to the cylinder head cooling system via the valve guide by the filled sodium. In the research results of Tanaka and Kawata [17], the maximum temperature of the HSV was 114 °C lower than the solid valve. It is true that lowering valve temperature only a slight amount may take it out of the critical range for failure.

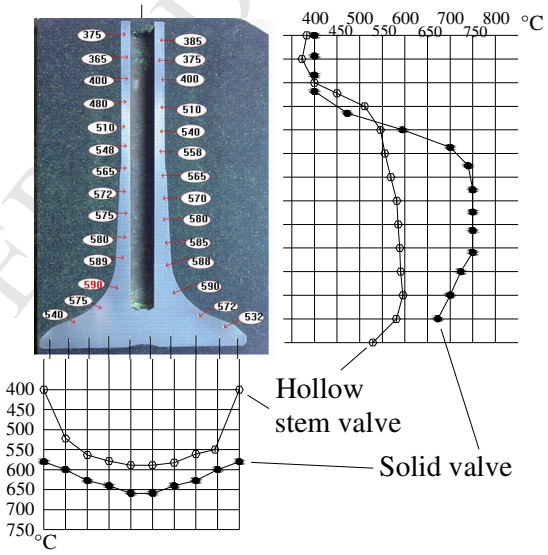

Fig.11. Comparisons of temperature distributions of solid valve and HSV (gasoline engine).

Table 5 Comparisons of results for solid valve and HSV (°C).

Type	Valve head	Valve surface	The highest of

	The highest	The lowest	The highest	The lowest	whole
Solid valve	665	575	745	400	745
HSV	581	400	590	lower than 375	590

For a conventional solid valve, most of the heat was transferred to the cooling system through the seat inserts, and the other was mainly through the valve guides [20]. Based on the presented experimental results and research presented in the literature [3, 5, 20], it is believed that the HHSV would have a better performance in temperature reduction. Due to the temperature reduction, engine designers could use less than half the amount of costly nickel as other high-temperature alloys, while providing comparable strength, wear and resistance. Also a decrease in the valve head temperature has a positive influence on valve-induced knocking behaviour [5]. It should be noted that the hardness method has some shortcomings. For example, it may even be uncertain which engine operating condition yields maximum temperature, because the corresponding test was only run at one steady state condition and did not provide temperature data throughout the engine operating range [19].

4.2 Fatigue behaviour

4.2.1 FEM stress analysis results

The FEM stress analysis results for the HHSV subjected to the load are presented in Fig. 12. It was found that, the maximum value in the von Mises stress distribution was 1.08 GPa when the load was set at 10 kN, and it exceeded the tensile strength of the 23-8N steel at 650 °C. When load decreased to 4.2 kN, the maximum von Mises decreased to 443 MPa, which still below the material tensile strength. The maximum von Mises occurred at the inner edge of the hollow cavity junction surface.

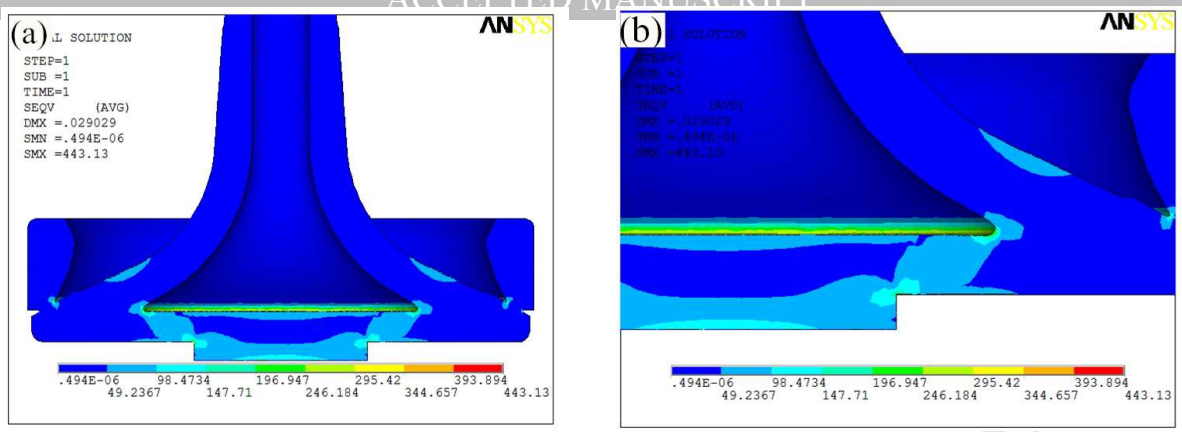

Fig. 12. Stress analysis results by FEM with a load of 4.2 kN.

4.2.2 RBF S-N curve

Based on the statistical lognormal distribution, the RBF results were analyzed and are illustrated in Fig. 13. According to the S–N equation and curve, the fatigue strength of the 23–8N steel was 345 MPa at 10^7 cycles at 650 °C.

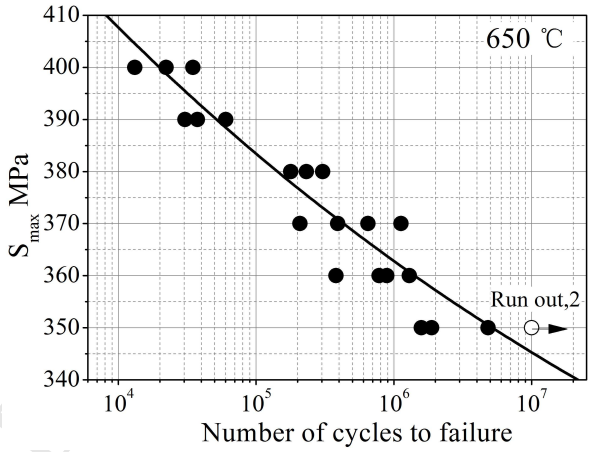

Fig. 13. S–N curves of 23-8N steel at 650 °C.

4.2.3 Durability of hollow head

The durability bench test results of four valves in the aspect of fatigue behaviour are presented in Table 6. As for 10 kN load, the valve 1 broken after 460×10^3 impact cycles with clearly cracks, as visible in Fig. 14. Due to the high contact force, the initial cracks in the valve head inner hollow cavity followed the friction welding position. The stress analysis by FEM pointed that

the maximum von Mises stress of the HHSV specimens occurred at the inner edge of the hollow cavity junction surface. However, the cracks of the valve head outside surface displayed differently. The position of the initial cracks was a little further away from the friction welding position. It could be inferred that the outside cracks were not affected by the friction welding area. As for 4.2 kN load, the hollow head of valve 2 still maintained integrated after ten million impact cycles. No cracks were found on the cross-sections of valve 2, as presented in Fig. 15. Based on the RBF material test results, FEM stress analysis results and valve components durability bench test results, it could be concluded that the design of the HHSV with current dimensions and materials has passed the durability assessment.

Table 6 Valve durability bench test results.

Specimen name	Valve type	Valve head material	Cycles (10^3)	Results
Valve 1	HHSV	23-8N	460	Broken
Valve 2	HHSV	23-8N	10,000	Run-out
Valve 3	Solid	X60	10,000	Run-out
Valve 4	HHSV	23-8N	10,000	Run-out

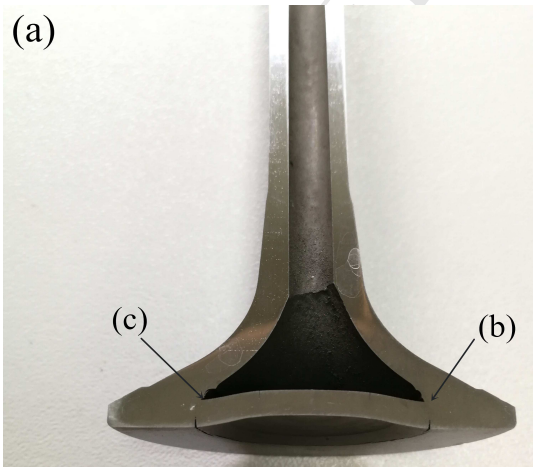

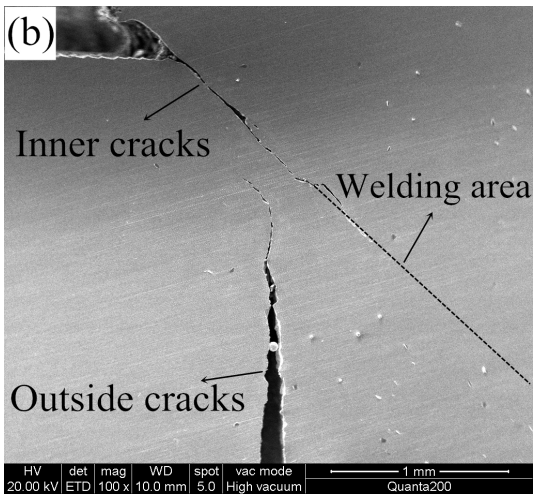

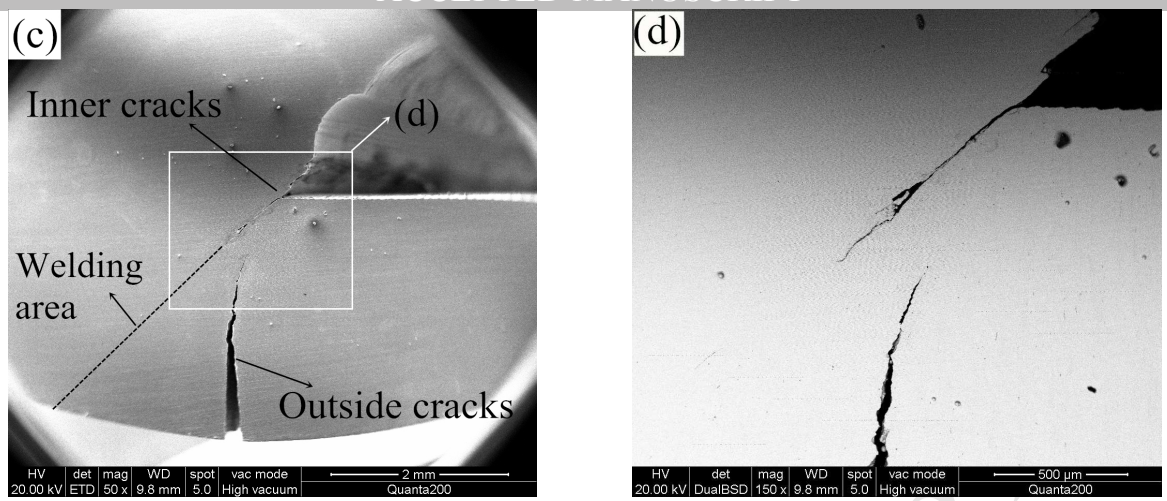

Fig. 14. Cross-sections SEM of valve 1 under 10 kN withstand 460×10^3 cycles

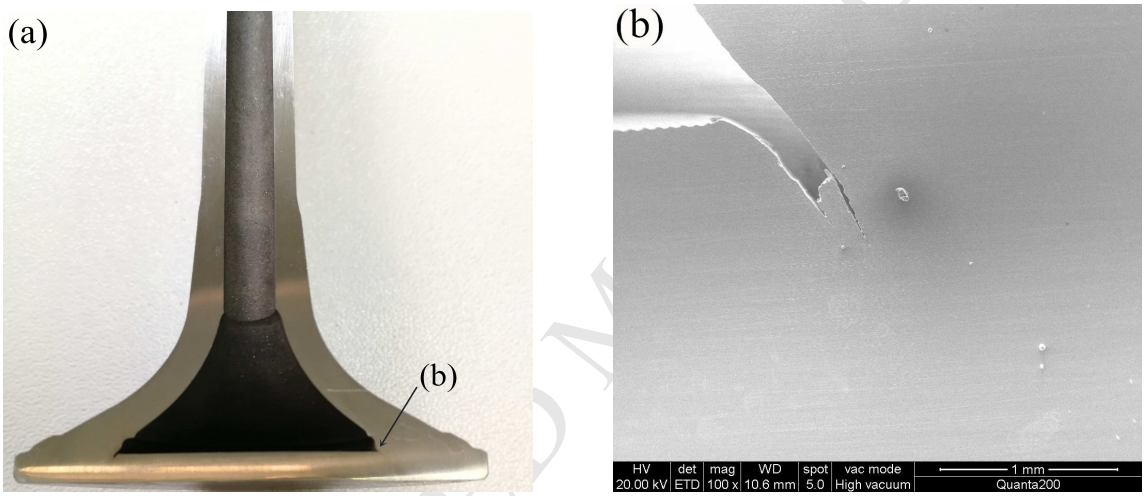

Fig. 15. Cross-sections SEM Valve 2 under 4.2 kN withstand $10{,}000\times10^3$ cycles

4.3 Wear resistance behaviour

4.3.1 Wear scar of valve seating face

The average valve seating face wear scar width versus the impact cycles is presented in Fig. 16, and Fig. 17 presents the wear scar area information. It is noticed that the wear scar width of valve 3 (solid valve) was the highest, showing the lowest wear resistance. Valve 4 wear scar width had a minimum value. Compared to the wear scar of valve 2 (nitrided 23-8N steel), the Stellite F hardfacing alloy on valve 4 performed better in terms of wear resistance ability.

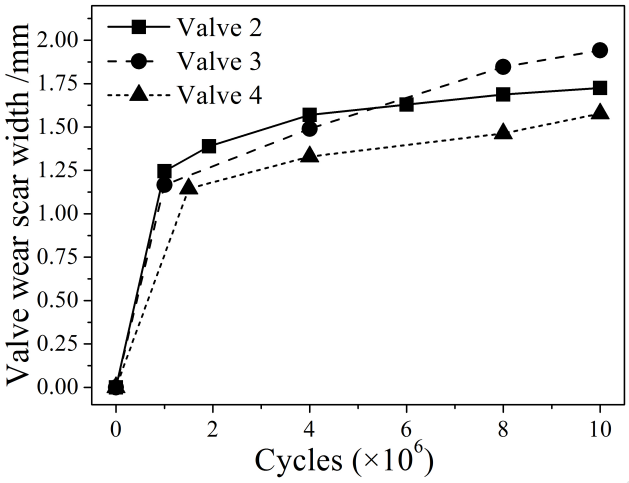

Fig.16. Average valve seating face wear scar width as a function of cycles.

The wear loss could be calculated from the wear scar area. Consequently, wear scar area information might be better for the wear resistance assessment. Fig. 17(a) presents worn profiles of the valve seating surface of the four valves. Every valve was measured four times at four points, error bar in the Fig. 17(b) represents the standard deviation of the wear scar area. Although valve 3 had the maximum value at wear scar width, it did not reach the maximum wear scar area value. In fact, valve 2 showed a higher wear loss than valve 3.

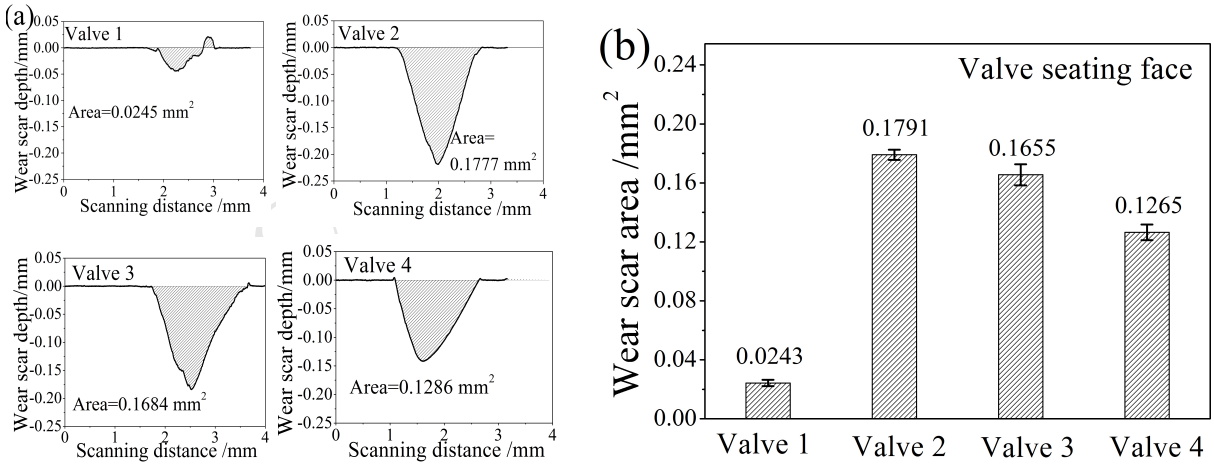

Fig. 17 (a) Wear scar profile of valve seating face; (b) wear scar area of valve seating face.

4.3.2 Wear scar of seat insert

Fig. 18(a) presents the wear scar for corresponding seat insert, the calculated results of wear scar

area is presented in Fig. 18(b). Seat insert 3 suffered the highest wear loss. It matched with a solid valve during the test, most of the heat from the valve was transferred to the cooling system through the seat insert. Consequently, it withstood apparently higher temperature than other seat inserts, which corresponded with the sodium valves, leading to an increase in wear loss. The total wear for each contact pair is presented in Fig. 19, and the valve recession is related to the total wear loss of every contact pair. It is found that the solid valve contact pair had a maximum total wear loss, the following was HHSV with 23-8N steel nitriding, the HHSV with Stellite F hardfacing alloy hold a minimum total wear loss. The presence of high melting point phases, such as carbide or ceramic compounds in hardfacing alloy is help preventing wear [21].

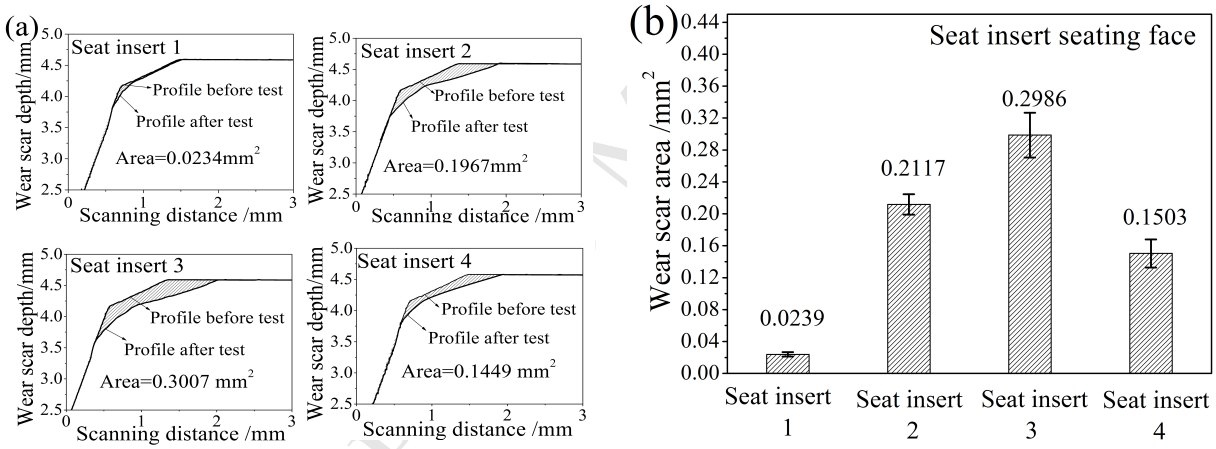

Fig. 18 (a) Wear scar profile of seat insert. (b) wear scar area of seat insert seating face.

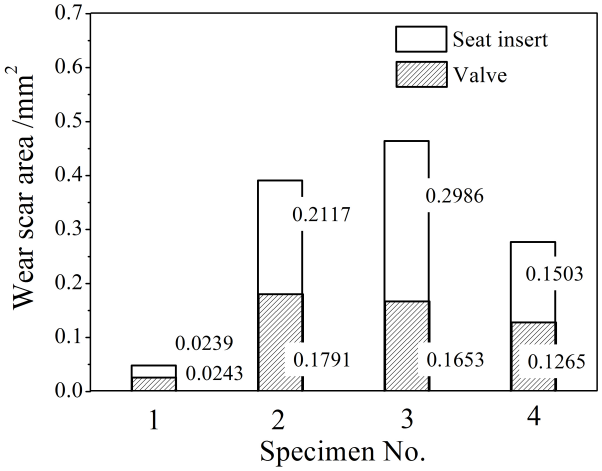

Fig. 19. Total wear of valve and seat insert.

4.4 Worn surface and wear mechanisms

4.4.1 Worn surface of valve seating face

Figs 20–22 presents the worn surface and cross-sections of the valve seating face of valves 1, 2 and 4, respectively. The EDS results of the areas on the valve seating faces are presented in Table 7. For instance, Fig. 20 presents the worn surface of valve 1 seating face. Severe plastic deformation was found at the edge of contact area, which was resulted from the large load. The EDS results (Table 7) of surface layers show that they contain high oxygen content. It is correlative with the elevated temperature test conditions, the debris generated from the closing impact began to oxidize, forming poorly adherent oxide layers.

Adhesive wear is characterized by bonding and subsequent breakage occurring alternately between sliding materials [21]. As the combustion pressure applies a load on the valve head, micro-sliding occurs on the interface of valve seating face and seat insert. Based on the research results of Forsberg et al. [22], sliding was a very important factor in the wear of heavy duty diesel valves. Adhesive wear characters were found on the worn surface of valve 2 seating face,

as presented in Fig. 21(b). It is possible that some adherent oxide layers was then detached or delaminated from the valve seating face surface as debris. Consequently, the wear mechanism evolution might be drawn, as it is in the literature [15], as wear due to the impact (impact wear) and sliding (adhesion and abrasion) in the contact, the rate of which is accelerated by as some type of oxidative wear due to the elevated temperatures. This indicates that there is no adverse wear mechanism initiated due to the design and manufacture of these valves.

Fig. 22(b) reveals the cross-section of the valve 4 seating face. No visible cracks were found in the subsurface of the wear scar of the two valves' seating faces, indicating that the material removal of the valve seating face was predominated by wear.

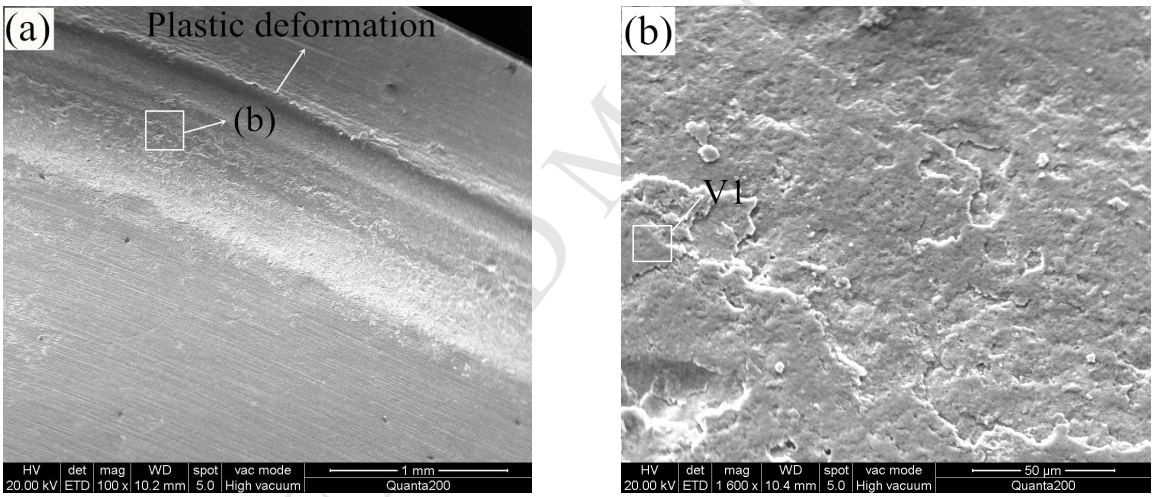

Fig. 20 (a), (b) Worn surfaces of valve 1 seating face and EDS test area V1.

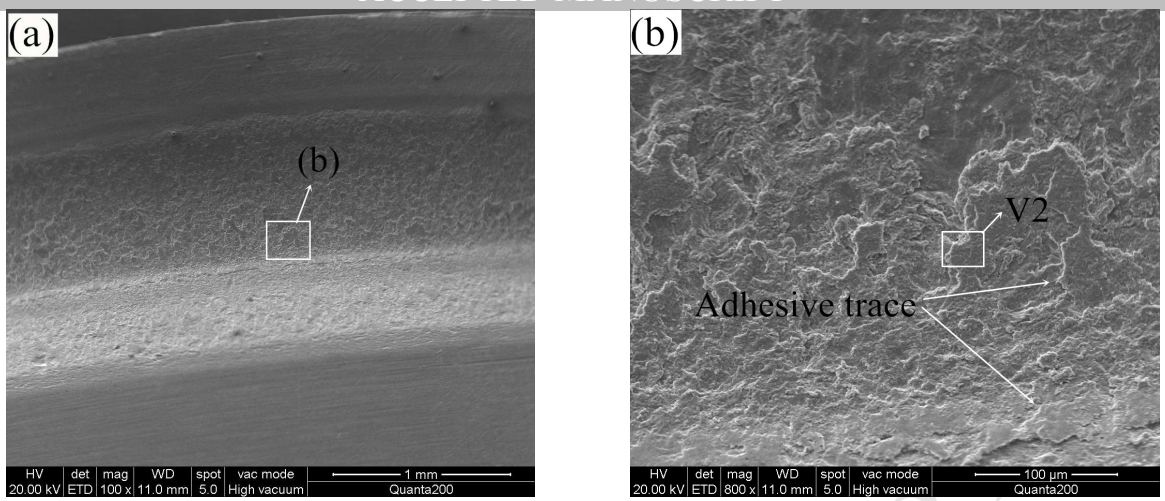

Fig. 21 (a), (b) Worn surfaces of valve 2 seating face and EDS test area V2.

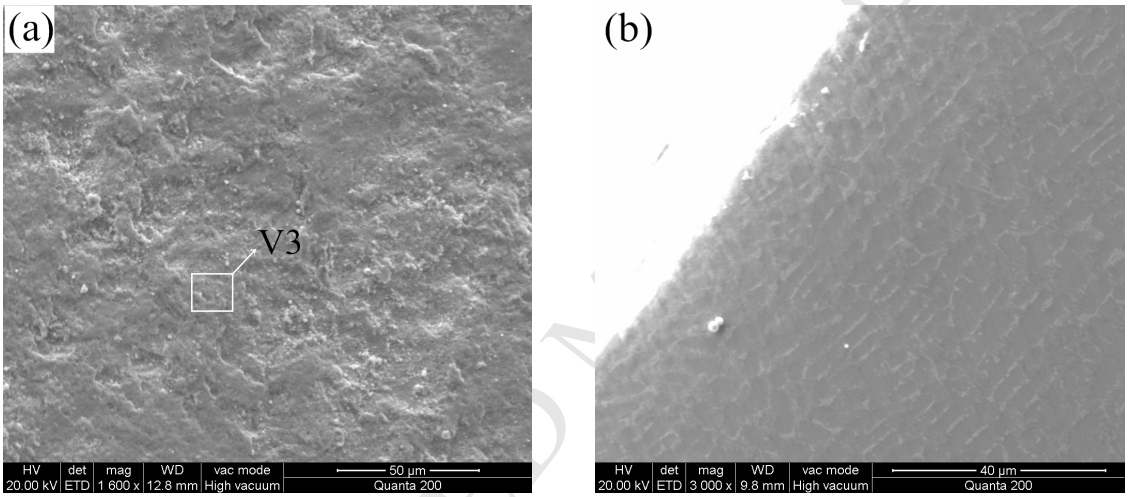

Fig. 22 (a) Worn surfaces of valve 4 seating face and EDS test area V3; (b) cross-section of valve 4 seating face.

Table 7 EDS results of the areas on valve seating face (wt. /%).

Specimen name	Area	Si	O	Al	Cr	Mn	Fe	Ni	Co	W
Valve 1	V1	1.37	32.3	–	14.97	1.48	47.20	2.69	–	–
Valve 2	V2	1.20	31.11	–	14.89	1.97	47.97	2.86	–	–
Valve 4	V3	0.85	25.48	1.37	17.09	2.04	18.65	10.91	14.21	9.4

4.4.2 Worn surface of seat insert

Worn surfaces of the four seat inserts are presented in Fig. 23–26. Adhesive traces could be

identified on the worn surfaces, and the surfaces are rough with small adhesion pits, especially at the edges of the seating faces. EDS results of the worn surfaces are presented in Table 8. Seat insert 1 held the minimum value in oxygen content, it could be due to the least test time. Seat insert 3 had the maximum value in oxygen content. Because it matched with a solid valve, compared to the sodium filled valve, more heat from the valve was transferred to the cooling system through the seat insert. Consequently, it is inferred that seat insert 3 was subjected to the higher temperature, leading to a higher oxygen content in its worn surface layers. Compared to non-contact area of seat insert 4, it is found that oxygen as well as cobalt were detected on the worn surface layers of seat insert 4. This means that the valve hardfacing alloy material was transferred to the seat insert surface and that the adhesion layers was an oxygen–rich compound.

In a real operation engine, protective tribofilms would be formed on the contact surfaces, the importance of this phenomenon, particularly for exhaust valve wear, was investigated experimentally by Forsberg et al. [23]. However, the test conditions during the durability bench test was a dry atmosphere, without the presence of oil, no tribofilms formed and thus no protection of the surfaces was given. Consequently, adhesive wear occurred on the both contact surfaces of the contact pair of valve and seat insert.

Lewis and Dwyer-Joyce presented a semi-empirical valve recession model. The model indicated that the major cause of valve recession was the impacts [15, 24]. As the impacts continue, flaking and depression of the contact surfaces occurred, as presented in Fig. 23 (b), Fig. 24 (b) and Fig. 26 (b). Cracks appeared on the layers, as presented in Fig. 25 (b). Consequently, the contact adhesion would be broken, and more likely due to the increased weakening of the surface

through oxidative wear, and fragments of material detach from the surfaces and act as debris (third bodies). The material removal resulted in valve recession.

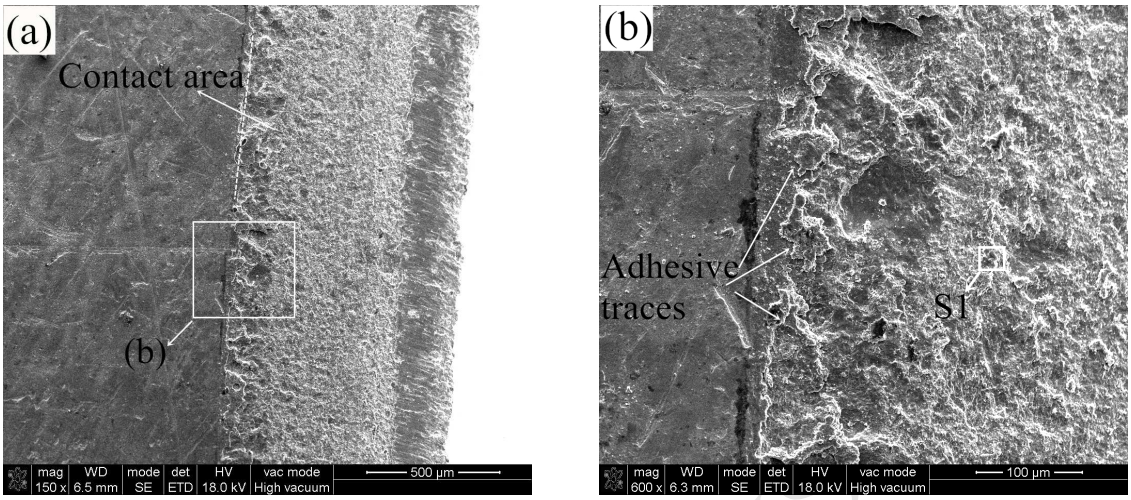

Fig. 23 (a), (b) Worn surfaces of seat insert 1 and EDS test area S1.

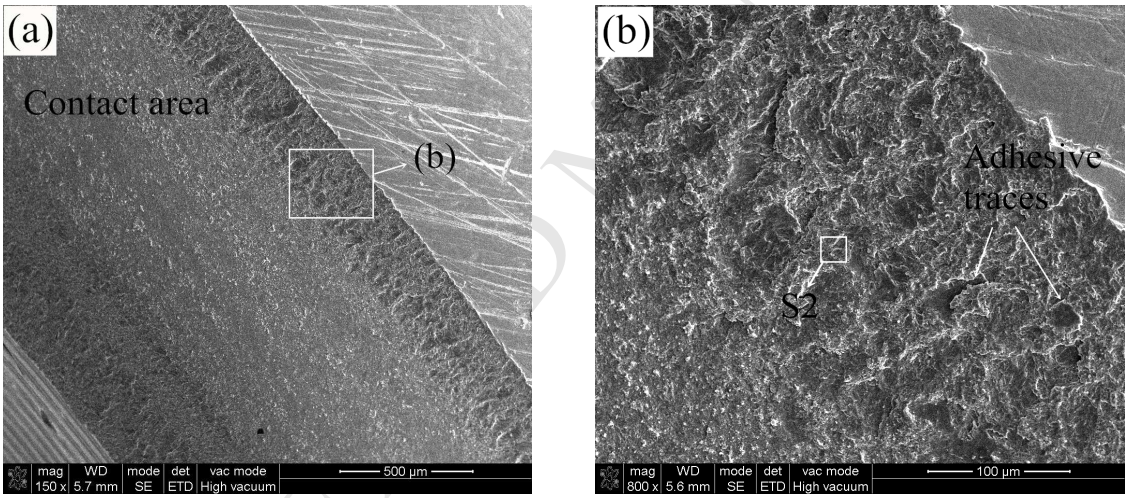

Fig. 24 (a), (b) Worn surfaces of seat insert 2 and EDS test area S2.

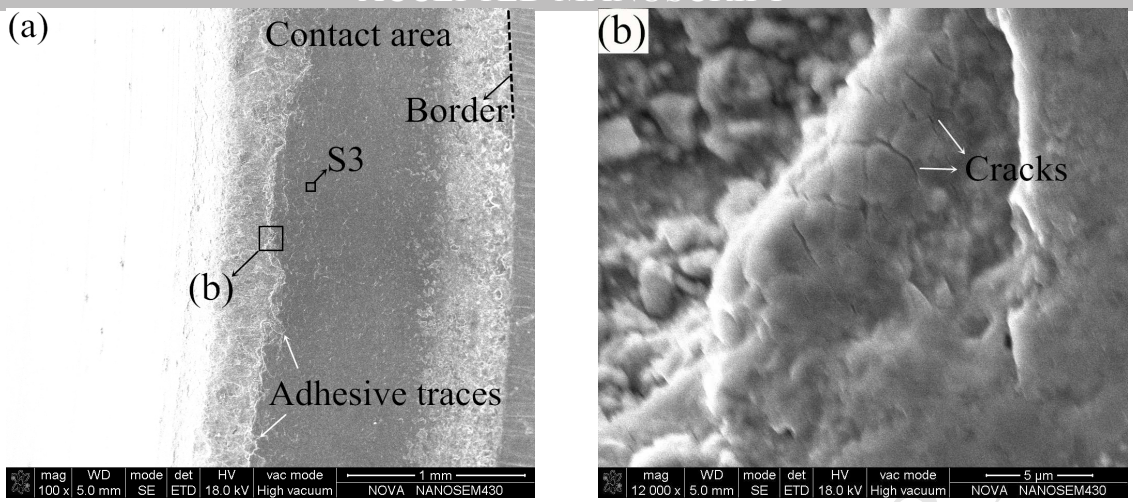

Fig. 25 (a), (b) Worn surfaces of seat insert 3 and EDS test area S3.

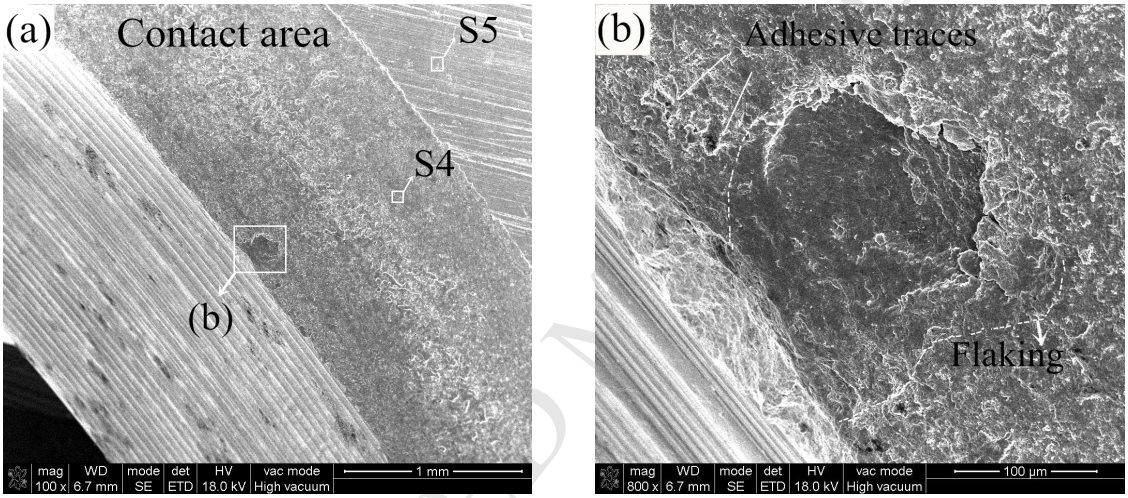

Fig. 26 (a), (b) Worn surfaces of seat insert 4 and EDS test area S4 of contact area, EDS test area S5 of non-contact area.

Table 8 EDS results of the areas on seat insert (wt. /%).

Specimen name	Area	C	Si	O	Cr	Mn	Fe	Ni	Co
Seat insert 1	S1	4.50	1.24	17.10	16.64	0.82	57.77	1.92	–
Seat insert 2	S2	4.07	1.15	19.18	18.43	0.87	53.85	2.46	–
Seat insert 3	S3	2.54	1.67	29.02	13.74	–	52.52	0.51	–
Seat insert 4	S4	4.32	1.44	25.54	12.77	0.64	45.53	3.49	4.11
Seat insert 4	S5	6.35	2.07	2.63	23.73	–	64.00	1.22	–

5. Future work

The fourth step of the drilling plus friction welding method presented in Section 2.2 is to produce the valve hollow stem by drilling, which requires high precision for production equipment. Furthermore, the drilling process was performed with low production efficiency and low utilization rate of material. A significantly efficient method will be introduced to produce the hollow stem of the valve through cross wedge rolling, as presented in Fig. 27. This method is named "cross wedge rolling plus friction welding method" and detailed information is presented in an authorized Chinese patent of the authors [25]. It has seven steps, as follows: (1) hollow pipe workblank preparation; (2) cross wedge rolling; (3) cutting; (4) shaping for valve hollow head; (5) friction welding sealing at valve hollow head; (6) sodium filling and friction welding sealing at valve hollow stem; (7) seating face hardfacing with Stellite alloy.

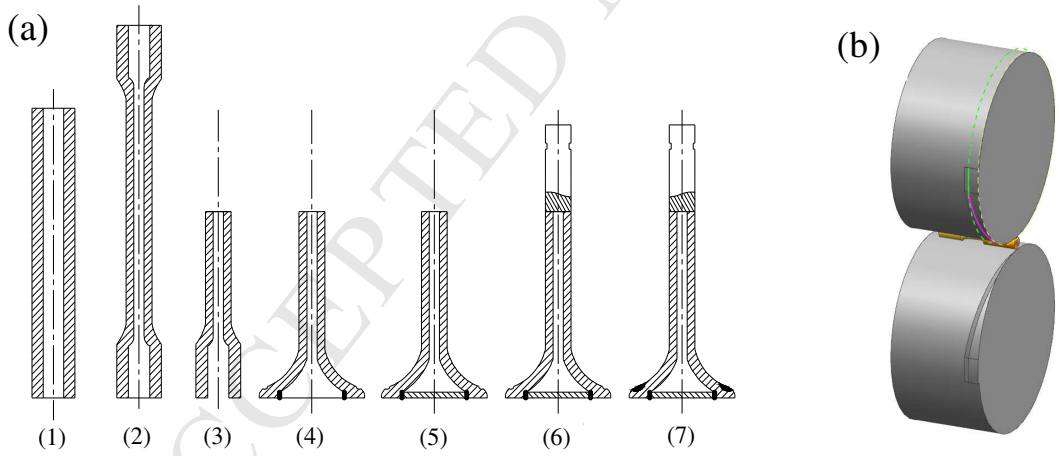

Fig. 27. (a) High efficient manufacture method with cross wedge rolling [25] (with the permission of reprinting from Mr. T. Zhang); (b) cross wedge rolling schematic.

6. Conclusions

A novel method for manufacturing hollow head & sodium filled engine valves is presented. The

manufacturing method is based on drilling and friction welding. Compared to the solid valve, the mass of the HHSV produced by the method was reduced by 16.1%. The assessment tests were performed to evaluate the durability of the hollow head and the wear resistance of the valve seating face. The conclusions can be drawn as follows.

(1) Compared to the solid valve, the highest temperature of the HSV was decreased from 745 °C to 590 °C.

(2) The current design for the valve hollow head passed the durability assessment test.

(3) The HHSV (made from 23-8N steel) on which the seating faces were hardfaced with stellite F had the best wear resistance. This type of HHSV could be a potential solution for a natural gas fuelled diesel.

(4) The wear mechanisms acting on the interface between the valve seating surface and the seat insert were found to be a combination of oxidative wear and adhesive wear. The wear loss was produced by impact (impact wear) and sliding (adhesion and abrasion).

(5) The high efficient manufacture method with cross wedge rolling process is also a potential manufacturing method to produce the hollow head & sodium filled valves.

Acknowledgements

The authors wish to thank Chairman Tao Zhang, Senior Engineer Dongqiang Mo, Wenlan Fu and Gang Chen and Engineer Qi Huang, Deci Kong and Feihua Wang from Huaiji Dengyun Auto–parts (Holding) CO., LTD. for providing the professional proposals for the paper. Mr. Jay Larson from Huaiji Engine Valve USA Inc. provided professional guidance for the paper. This study was sponsored by the Guangdong Province Scientific and Technological Projects (No.

2016KZ010104). The authors acknowledge the financial support from the China Scholarship Council (CSC). This work was also supported by YangFan Innovative & Entrepreneurial Research Team Project (No.201312G02).

Conflicts of Interest: The authors declare no conflict of interest.

References

[1] Lai FQ, Qu SG, et al. Design and operation of a new multifunctional wear apparatus for engine valve train components. Proc IMechE, Part J: J Engineering Triblogy 2018; 232(3): 259–276.

[2] Wang YS. Introduction to engine valvetrains. Warrendale: SAE International; 2007.

[3] Colwell AT. Corrosion-resistant metals for valves and seats on heavy-duty engines. SAE 480178, 1948.

[4] Hu XG. The hollow engine valve and its manufacturing technology. Internal Combustion Engine Parts 2002; 5:13–19[in Chinese].

[5] Baek HK, Lee SW, Han D, et al. Development of valvetrain system to improve knock characteristics for gasoline engine fuel economy. SAE 2014–01–1639, 2014.

[6] Starr F. Design and development of exhaust valves for internal combustion engines from the perspective of modern thinking: Part 2 1930–90. Int. J. for the History of Eng. & Tech. 2014; 84(1): 1–29.

[7] Starr F. Design and development of exhaust valves from the perspective of modern thinking: part 3: reverse engineering of American and British sodium-cooled valves. Int. J. for the History of Eng. & Tech. 2016; 86(1): 70–92.

[8] Heron SD. Exhaust-valves and guides for aircraft engines. SAE 240033, 1924.

[9] Wang HJ. The Forging Technology for hollow head exhaust valves. Hot working technology 1981;3: 24–30 [in Chinese].

[10] Beerens C, Mueller A, Karrip K. Transient valve temperature measurement (TVTM). SAE 2017-01-1066, 2017.

[11] Cooper D, Thornby J, Blundell N, et al. Design and manufacture of high performance hollow engine valves by Addictive Layer Manufacturing. Materials and Design 2015; 69:44–55.

[12] Zhang ZR, Sun YS, Lin XJ, et al. A forming technology for hollow head & sodium filled engine valve which based on cross wedge rolling to produce workblank. China patent, ZL 201510236950.9. 2017-10-27 [in Chinese].

[13] Peng HX, Wang XH, Chen C, Chen W. Development of engine valve and seat ring strengthening wear test system. Railway Locomotor & Car 2011; 31: 296–298 [in Chinese].

[14] Forsberg P, Gustavsson F, Hollman P. Jacobson S. Comparison and analysis of protective tribofilms found on heavy duty exhaust valves from field service and made in a test rig. Wear 2013; 302: 1351–1359.

[15] Lewis R, Dwyer-Joyce R.S. Investigation of wear mechanisms occurring in passenger car diesel engine inlet valves and seat inserts. SAE 1999–01–1216, 1999.

[16] Wang YS, Narasimhan S, Larson JM, Larson JE. Barber GC. The effect of operating conditions on heavy duty engine valve seat wear. Wear 1996; 201:15–25.

[17] Tanaka N, Kawata A. Measurement technique of exhaust valve temperature. SAE 2015-01-1999, 1999.

[18] Wisniewski TS. Experimental study of heat transfer on exhaust valves of 4C90 diesel

engine. SAE 981040, 1998.

[19] Savel III FJ, Gavrilesscu A. Live engine heat flow from intake valve centerline to coolant passage using 8 thermocouples in series with various materials. SAE 2002-01-0711, 2002.

[20] Baniasad MS. Khalil E, Shen F. Exhaust valve thermal management and robust design using combustion and 3d conjugate heat transfer simulation with 6-sigma methodology. SAE 2006-01-0889, 2006.

[21] Wang YS, Schaefer SK, Bennett C, Barber GC. Wear mechanisms of valve seat and insert in heavy duty diesel engine. SAE 952476, 1995.

[22] Forsberg P, Debord D, Jacobson S. Quantification of combustion valve sealing interface sliding-A novel experimental technique and simulations. Tri. Int. 2014; 69: 150–155.

[23] Forsberg P, Elo R, Jacobson S. The importance of oil and particle flow for exhaust valve wear - An experimental study. Tri. Int. 2014; 69: 176–183.

[24] Lewis R, Dwyer-Joyce R.S. Wear of diesel engine inlet valves and seat inserts. Proc IMechE, Part D: J Automobile Engineering 2002; 216: 205–216.

[25] Zhang T, Zhang ZR, Mo DQ, et al. A hollow head & sodium filled engine valve which based on cross wedge rolling to produce workblank. China patent, ZL 201510237591.9. 2017-11-28 [in Chinese].

Research Highlights

A new manufacturing process for hollow head & sodium filled valves (HHSVs).

The durability tests were conducted using bespoke bench-top apparatus.

The material loss magnitude of HHSVs were compared to the solid valve.

The temperature distributions comparison of solid valve and hollow stem valve.

The valve and seat insert wear mechanisms are oxidation accelerated adhesion.